TRENDS IN SCIENCES 2024; 21(6): 7604 RESEARCH ARTICLE
https://doi.org/10.48048/tis.2024.7604

Arsenic Adsorption Isotherms of Sediments from Old Mining Area and Their Implications: A Case Study of the Ron Phibun Area, Thailand

Suma Nookaew[1], **Chuthamat Rattikanukha**[3,4],
Kittipong Kunchariyakun[1,4,*] **and Chairat Siripatana**[1,2]

[1]*School of Engineering and Technology, Walailak University, Nakhon Si Thammarat 80160, Thailand*
[2]*Biomass and Oil-Palm Excellence Center, Walailak University, Nakhon Si Thammarat 80160, Thailand*
[3]*School of Languages and General Education, Walailak University,*
Nakhon Si Thammarat 80160, Thailand
[4]*Center of Excellence on Disaster Sustainable Management, Walailak University,*
Nakhon Si Thammarat 80160, Thailand

([*]Corresponding author's e-mail: kunchariyakun.k@gmail.com)

Received: 12 October 2023, Revised: 14 November 2023, Accepted: 21 November 2023, Published: 10 April 2024

Abstract

Although tin mining activities in the southern part of Thailand have been abandoned for more than 40 years, arsenic contamination in old tin-mining areas continues to pose a health risk. Fortunately, natural adsorption of arsenic by sediment has reduced the arsenic concentration in water to the maximum allowable level within a 10-kilometre radius of the mine sources. This article attempts to characterize the arsenic adsorption properties of sediment along a water creek which passes through the old tin-mine areas in Ron Phibun district, Nakhon Si Thammarat province, Thailand, where the contamination has been most severe. It was found that Fe tends to be associated with the adsorption capacity of arsenic in sediment. However, pH 4 and pH 7 did not associate with adsorption capacity. At pH 12, the solubility of arsenic increases, making it less likely to be adsorbed into the sediment and more likely to dissolve in water. For the adsorption isotherms of the sediment, the so-called '2-step Langmuir/Freundlich models', with the advance of switching functions (Logistic or Arctan functions), were proposed. Then, based on the principle of parsimony, a stepwise model reduction approach was used to choose the optimal models. It was found that the isotherms were used successfully to describe the historical arsenic-contamination data of the past 14 years (2005 - 2019) and to predict future trends qualitatively.

Keywords: Arsenic adsorption, Sorption isotherms, Sediments, Old mining, Water pollution, Two-step Langmuir model, pH, Iron

Introduction

Contamination by arsenic (As) in Thailand was first recognized in Ron Phibun District, Nakhon Si Thammarat Province, in 1987. People living near or in the old tin-mine area were sick, their skin became black, and they were diagnosed with skin cancer [1,2]. Ron Phibun is located in the Southeast Asian Tin Belt, and was an area for tin production before its closure in 2004. As has been released from prior bedrock and alluvial mining of tin during the last century. Both surface water and groundwater surrounding the mining sites contained very high levels of As (and gt; 580 μg/L for surface water and up to 5,100 μg/L for shallow groundwater) [3-5]. Although the tin mining area was closed in 2004 [6], the contaminant monitoring program conducted by the Department of Mining Industry (1992 to the present) has shown that the level of arsenic contamination from these old mines still poses a high risk to people who live near the water-way which runs 100 km downward from the abandoned tin mines. Natural wash-away and As-redeposits only reduce the As concentration in the waterway very slowly. Elimination of the current risk in the next few decades is not feasible because of the excessively high cost of remediation [7].

As is one of the most toxic heavy metal present worldwide in minerals, soils and water resources. AIt is also transportable and difficult or costly to remove. In general, As in inorganic forms are more toxic than organic forms and extremely hard to eliminate. As exists predominately in the forms of inorganic As(III) and As(v) in most types of soils and sediments, and the toxicity and mobility of As(III) is greater than those of As(V) [8,9]. As-contaminated water sources alone have affected the health of approximately 150 million people worldwide [10,11]. The spread of As into water resources is through different paths, including air, food, industries, mining and the contaminated water, soils and sediments [12,13]. The symptoms of long-term exposure to inorganic As include dermal neurological, hematological, gastrointestinal, hepatic, renal, cardiovascular, and respiratory diseases, and diabetes mellitus, which can cause brain malfunction in children and adults [14]. According to EU Council, WHO, US EPA and ATSDR, drinking water should contain As concentration less than 10 $\mu g/L^{-1}$ [15-18]. Recent research and publications follow this trends albeit more focus on developing new adsorbents and processes to remediate the on-going As contamination in soils and water resources [19]. It is well recognized that adsorption is the most effective technology for As removal from the contaminated water sources [20]. The recent development is moving toward metal-organic frameworks (MOFs) [21-23], Chitosan and its derivatives [24,25], layered double metallic hydroxides (LHDs) [26,27], Bio-char and other complex materials as adsorbents for heavy metals, particularly As(III) and As(V). The understanding of the mechanisms of As adsorption and their related transport phenomena has increased significantly from the last decade until now [10,25]. In the current knowledge, the adsorption mechanism for arsenic includes surface complexation, electrostatic attraction, redox and coordination. In addition to pH, dissolved organic matter (DOM), particularly organic acids and Fe-complexes which are closely related to each other, together influence the fluidity and migration [10]. According many reports, the migration extent of As in water and soil is strongly associated to (hydro)oxides, which is considered as the main As-bearing minerals [9,28].

Furthermore, there has not been any attempt to describe quantitatively the spread of As starting from the tin mines down the water way until it reaches the sea. It is possible to predict the future trends of As concentration statistically from the monitored data but the statistical approach would be limited to the prediction of the trend with little mechanistic understanding. Thus, comprehensive models are required to represent and describe these complex phenomena in terms of chemical factors (pH, the presence of Fe/Mn ion, colloids and Eh), and physical factors (seasoning water speed, mass transfer, mixing, etc.).

Most of the studies on sorption isotherms of arsenic for different kinds of adsorbents concluded that the Langmuir and Freundlich models are sufficient to describe the effect of As concentration on the surface loading of As(III) and As(V) on the adsorbent samples [29]. The following forms for Langmuir and Freundlich isotherms were used widely [21].

$$q_e = q_m \frac{C_0}{1 + bC_e} \tag{1}$$

$$q_e = K_F \, C_e^{n/1} \tag{2}$$

where q_e, C_e, q_m, C_0 and b are equilibrium concentration in the adsorbent (mg/kg), equilibrium concentration in the liquid phase (mg/L), adsorbent maximum capacity of absorbent (mg/kg), initial concentration (mg/L) and a Langmuir parameter, respectively. K_F and n are Freundlich parameters.

Other forms of isotherms (e.g. Temkin, Radushkevich and Redlich-Peterson isotherms) were tested for As-water-soil and related systems but the goodness-of-fit to various equilibrium data sets was not significantly better [22,23,30,31]. Moreover, it appears that the adsorption equilibrium of As-water-soil and related systems has multi-layers and multi-modes (mechanisms) which often make Langmuir and Freundlich isotherms incapable of describing the full-range of the data [32-35].

This work is a fundamental step in our attempt to develop a mechanistic model to describe and predict the spread and relocation of As along the water pathway in the area mentioned earlier, based on the so-called volumetric dispersion [36]. Due to the complex nature of desorption/adsorption of As, particularly the sediment under/along the water pathway, as well as the soil movement or the sedimentation of the sediment, it is not feasible to formulate a comprehensive mathematical model to describe the dynamics of As contamination as in the current case without this important step. Thus, this article investigates the complexity of the problem by characterizing the desorption/adsorption of As in the sediments which play a significant role in limiting the spread of As and the equilibrium relation called the “sorption isotherm” for 4 pairs of As-sediments. These isotherms were then used to interpret some samples of As monitoring data in the Ron Phibun basin. The main objective of this article is to provide a fundamental understanding of how these sediments behave when they make contact with water contaminated with As at different concentrations and pH. The goal is to represent and predict the contaminating phenomena as well as how the contaminant is absorbed or reacts which renders it less toxic as a function of distance and time as well as other physical chemical properties of water and sediment.

Materials and methods

Study area

An old mining area in Ron Phibun was investigated to develop adsorption isotherms of As-water-sediment systems. The old-mining area and creeks are located in the Ron Phibun District, Nakhon Si Thammarat. The site is located at 8°04' - 8°14' latitude, 99°46' - 99°54' longitude, at the foot of the Ronna-Suanjan mountains, 26 km southwest of the city of Nakhon Si Thammarat. **Figure 1** shows the route from the old-mining area to the Pakphanang estuary. The study area is at Hwuay Hua II which includes Station 1 (St 1, Huay Huamhuang), Station 2 (St 2, Stadium), Station 3 (St 3, Huay Ronna), Station 4 (St 4, Huay Namkhun), Station 5 (St 5, Huay Namchan), Station 6 (St 6, Muang Ngam) and Station 7 (St 7, Teppanomchuad Temple). The water flows in the study area past the mine closure to where the ore residues from the tin dressing processes were dumped. Thus, a large amount of As-contaminated residues was covered under a thin layer of surface sediment.

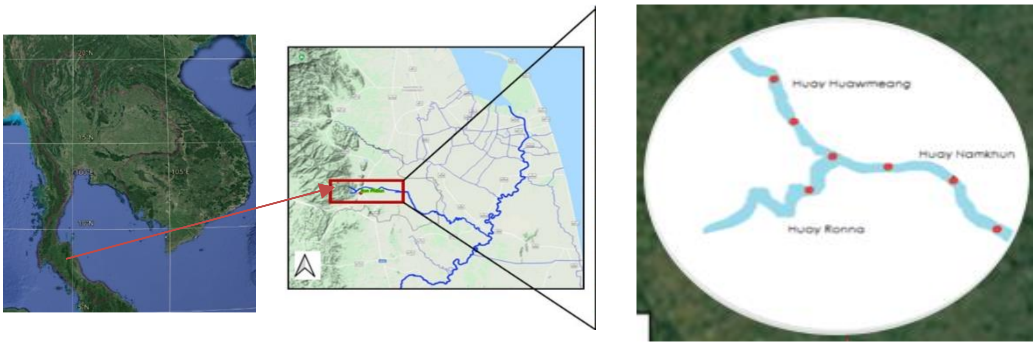

Figure 1 Map of the study area in the Ron Phibun District.

Batch adsorption experiments

Analysis of arsenic and iron in sediment

The 7 sediment samples were collected from the old-mining area in the Ron Phibun District, Nakhon Si Thammarat. The samples weighed (20 g) and sieved by using a 200-mesh (0.075 mm aperture). The samples were preserved at room temperature (25 - 30 °C). Then, 1 g of the samples (particle size < 1 mm) were digested by using 10 mL of the mixture of 70 - 72 % perchloric acid and 65 % nitric acid ($HClO_4$:HNO_3 2:1) at 85 ± 5 °C for 5 h (adapted from [30,37]). The As and Fe concentrations were analyzed using ICP-OES (inductively coupled plasma-optical emission spectrometry, Perkin Optima 3300 DV) [38]. All analyses were conducted in a triplicate manner.

Experiments of batch adsorption/desorption in sediment

The sediment samples (2 g) from Huay Huamhuang, Stadium, Huay Ronna and Huay Namkhun were screened to a particle size of < 2 mm (100 mesh screening). Fifty mL of 0.05 mol NaCl with a predetermined amount of As (0, 10, 25, 50, 100, 150 and 200 ppm) was added into the sediment and the mixtures were placed in a shaking incubator at ambient temperature (28 ± 1 °C) for 1,440 min. The pH was controlled by adding sulfuric acid or sodium hydroxide solution depending on the required pH of the samples (pH 4, 7 and 12). During the batch adsorption/desorption, the shaker was stopped at 10, 20, 30, 60, 90, 120, 240, 360, 480, 900 and 1,440 min and the samples were taken out at the predetermined process times. Then, the samples were centrifuged at 16,000 rpm for 10 min [39]. The clear solution was analyzed for As using ICP-OES (inductively coupled plasma-optical emission spectrometry, Perkin Optima 3300 DV). All experiments were carried out in a triplicate manner.

Determination of the equilibrium As-concentrations in the liquid phase and their corresponding As density in the sediments

The adsorption of each batch was measured, the 1st-order long-term trend of the As concentration in the liquid phase was taken as the equilibrium concentration. That is:

$$C_e = C_0 + ae^{-bt} \tag{3}$$

The corresponding As concentration in solid phase was calculated by material balances.

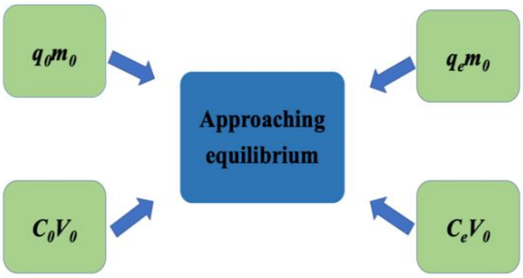

Figure 2 The material balances of the batch adsorption experiments.

After the batch adsorption the process was allowed to proceed until an equilibrium condition was achieved and the solid and liquid phases were separated. Then the equilibrium concentration in the liquid phase was analyzed. The As density in the solid phase at equilibrium can be calculated by the following equation.

$$q_e = \frac{V_0}{M_0}(C_0 - C_e) + q_0 \tag{4}$$

where q_0 and q_e are As densities in solid phases at initial time and at equilibrium, respectively. Similarly, C_0 and C_e are the corresponding As concentrations in the liquid phase. V_0 is the liquid (water) volume (l) used in the batch adsorption, and M_0 is the mass of the solid phase (kg).

Results and discussion

Adsorption isotherms of As in sediments

According to IUPAC (International Union of Pure and Applied Chemistry), the classification of adsorption isotherms is used to classify the different types of isotherms based on the shape of the curve that describes the relationship between the amount of adsorbate and the amount of adsorbent. The typical sorption isotherms can be categorized into 5 types which are: Type I (Langmuir isotherm) characterized by a linear relationship between the amount of absorbate and the pressure at constant temperature, type II (Freundlich isotherm) characterized by a non-linear relationship between the amount of absorbate and the pressure at a constant temperature, type III (Temkin isotherm) characterized by the natural logarithm of the amount of adsorbate and the reciprocal of the temperature at constant pressure, type IV (BET isotherm) characterized by a linear relationship between the natural logarithm of the number of the adsorbate and the pressure at constant temperature, type V (Horizontal isotherm) characterized by a horizontal portion at high coverage, indicating that the adsorbent has reached its maximum adsorption capacity and additional adsorbate cannot be adsorbed [40]. It is important to note that most of the absorbents do not show a perfect fit to any isotherm and that they can exhibit more than 1 type. Therefore, multiple isotherm models are used to describe the adsorption process and compare the best-fit model based on the experimental data.

Most of the studies on the sorption isotherms of arsenic for different kinds of adsorbents concluded that the Langmuir and Freundlich models are sufficient to describe the effects of As concentration on the surface loading of As(III) and As(V) on the adsorbent samples [41]. The following forms for Langmuir and Freundlich isotherms were used widely [31]. The equation of Langmuir isotherms is:

$$q_e = q_m \frac{C_0}{1+bC_e} \tag{5}$$

where q_e, C_e, q_m, C_0 and b are equilibrium concentration in the adsorbent (mg/kg), equilibrium concentration in the liquid phase (mg/L), adsorbent maximum capacity of absorbent (mg/kg), initial concentration (mg/L) and a Langmuir parameter, respectively. The equation of the Freundlich isotherm is:

$$q_e = K_F \, C_e^{n/1} \tag{6}$$

where K_F and n are Freundlich parameters, other forms of isotherm (e.g. Temkin, Radushkevich and Redlich-Peterson isotherms) were tested for As-water-soil and related systems but the goodness-of-fit to various equilibrium data sets was not significantly better [29,42-44]. Moreover, it appears that the adsorption equilibrium of As-water-soil and related systems has multi-layers and multi-modes (mechanisms) which often make the Langmuir and Freundlich isotherms incapable of describing the full-range of the data [32-35].

The two possible extensions of Langmuir and Freundlich isotherms

As a result of these preliminary reviews, the traditional Langmuir and Freundlich isotherm may not be suitable for describing most of the As-water-soil equilibrium data for a wide range of As concentrations ($0 < C_e < 200$, $0 < q_m < 2{,}000$ ppm). Thus, the following 2-step models are proposed. Essentially, they are extensions of the traditional Langmuir and Freundlich isotherms modified to accommodate 2 consecutive adsorption mechanisms.

Two-step Langmuir isotherm (TSL isotherm)

This model tries to mimic 2 sorption isotherms in which one is imposed on top of the other due to increased adsorption capacity. As the concentration of adsorbate becomes high enough, a different type of adsorption mechanism is induced which increases the adsorption capacity to another level. For simplicity and flexibility, the following empirical form is based on the Langmuir isotherm and Logistic functions as follows.

$$q_e = \frac{q_c b_1 C_e}{1+b_1 C_e} + \frac{q_m - q_c}{1+exp(-k(C_e - C_{ec})+a)}\frac{b_2 C_e}{1+b_2 C_e} \tag{7}$$

where q_e, C_e and q_m are the equilibrium concentrations in the adsorbent (mg/kg), the equilibrium concentration in the liquid phase (mg/L) and the adsorbent maximum capacity of the absorbent (mg/kg).

q_c and C_{ec} are the critical adsorption capacities and their corresponding critical adsorbate concentrations in the liquid phase which is characterized by the lower end of the isotherms (mg/g).

b_1 and b_2 are the Langmuir parameters for the lower and upper regions of the sorption isotherm, respectively.

The term $1/\left(1 + exp(-\kappa_l(C_e - C_{ec}) + a)\right)$ is the unit Logistic equation. $exp(a)$ is the coefficient of the exponential term. The Logistic term of the TSL isotherm not only has mechanistic implications, but it is also used as a switching (C_{ec} or preference) function. That is, it joins the 2 Langmuir isotherms which dominate at different As concentrations into a continuous unified isotherm. This switching function is characterized by how the behavior of adsorption changes as the adsorbate concentration increases. If $k = 0$, both adsorption mechanisms are visually inseparable, but if $k \to \infty$ the change from 1 mechanism (at low adsorbate concentration) to another one (at high adsorbate concentration) is abrupt as the adsorbate increases past C_{ec}. Another popular switching function is the arctan function of the following form.

$$(1/\pi)\left(\tan^{-1}\left(\kappa_a(C_e - C_{ec})\right) + \pi/2\right) \tag{8}$$

In a later discussion, we describe this function as the "arctan switching function" which can replace the Logistic function as an alternative switching function. However, the Logistic function is preferred when it is applicable because of its mechanistic meaning as will be discussed in section 8. In Eq. (8), κ_a is the switching parameter for the arctan function in the same way as κ_l is to the Logistic function.

Two-step Freundlich isotherm (TSF isotherm)

Similarly, based on Freundlich isotherm, we obtain the following form of 2-step Freundlich isotherm

$$q_e = q_c C_e^{1/m} + \frac{q_m - q_c}{1 + exp(-k(C_e - C_{ec}) + a)} C_e^{1/n} \tag{9}$$

where q_c, q_m and n are parameters of the model which can be described in a similar way as in the 2-step Langmuir isotherm.

Langmuir-Logistic isotherm (LL isotherm)

If the Langmuir component in the 2nd term of the TSL model does not make a significant contribution in explaining the experimental data, the TSL model should be reduced to the LL model which has the following form.

$$q_e = \frac{q_c b_1 C_e}{1 + b_1 C_e} + \frac{q_m - q_c}{1 + exp(-k(C_e - C_{ec}) + a)} \tag{10}$$

In this model, the role of the logistic term does not only have a switching function, but, by itself, it also describes the equilibrium pattern of the upper end of the isotherm.

Freundlich-Logistic isotherm (FL isotherm)

Similarly, if the contribution of the Freundlich component in the TSF model is not statistically significant, it should be reduced to the FL model which has the following form.

$$q_e = q_c C_e^{1/m} + \frac{q_m - q_c}{1 + exp(-k(C_e - C_{ec}) + a)} \tag{11}$$

The role of the logistic term is the same as that in the LL model.

The mechanistic description of the Logistic equation in the context of As adsorption

Pierre-Francois Verhulst (1804 - 1849), a Belgian mathematician, was the 1st author who introduced the logistic function as a model for population growth in 1838. It was used to describe the self-limiting growth of a population [45,46]. It is also called 'Verhulst's equation'. In the context of As adsorption, it can be reformulated as the following.

Consider As concentration in liquid solution as the independent variable and As in the adsorbent as the dependent variable:

$$\frac{dq_e}{dC_e} = kq_e \frac{(q_m - q_e)}{q_m} \tag{12}$$

where k is the gradient coefficient of the adsorption, characterizing the relative affinity of the adsorbate toward the adsorbent. High k indicates a strong affinity toward the adsorbent, or the equilibrium is highly preferable for the adsorbent.

The term on the left-hand side dq_m/dC_e is the gradient of the adsorption isotherm at any concentration of As in the solution. The q_m is the maximum adsorption capacity of the adsorbent. The term $(q_m - q_e)/q_m$ is the fraction of the remaining capacity of the absorbent. Eq. (12) states that the gradient of adsorption isotherm is proportional to the in-solid adsorbate concentration times the remaining fraction of the adsorption capacity. Starting from the initial value of C_e, as q_e increases the gradient (slope of the adsorption isotherm as shown in **Figure 3**) until it reaches the point of maximum gradient, then it levels off and approaches 0 for a very high value of C_e.

The solution of Eq. (13) is:

$$q_e = \frac{q_m}{1 + exp(-k(C_e) + a)} \tag{13}$$

where a is a constant which is represented by the isotherm along the C_e axis, the logistic equation (Eq. (13)) has a sigmoid shape which can be used as a switching function. At the same time, its physical meaning is intuitive. It is thus a preferable choice for extending both Langmuir and Freundlich isotherms to types-IV and -V sorption isotherms.

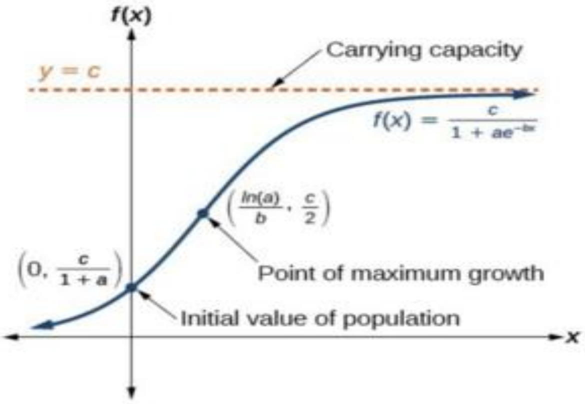

Figure 3 A representation of the gradient changes over C_e according to the logistic model.

A general scheme to obtain a parsimonious model from a general form of the 2-step Langmuir isotherm

To obtain a parsimonious model, all parameters should be tested for statistical significance or at least they should obviously contribute to the fundamental meaning. The strategy for the TSL isotherms can be visualized as in **Figure 4**. A similar strategy is applied to the TSF isotherms by replacing the Langmuir terms with the Freundlich terms.

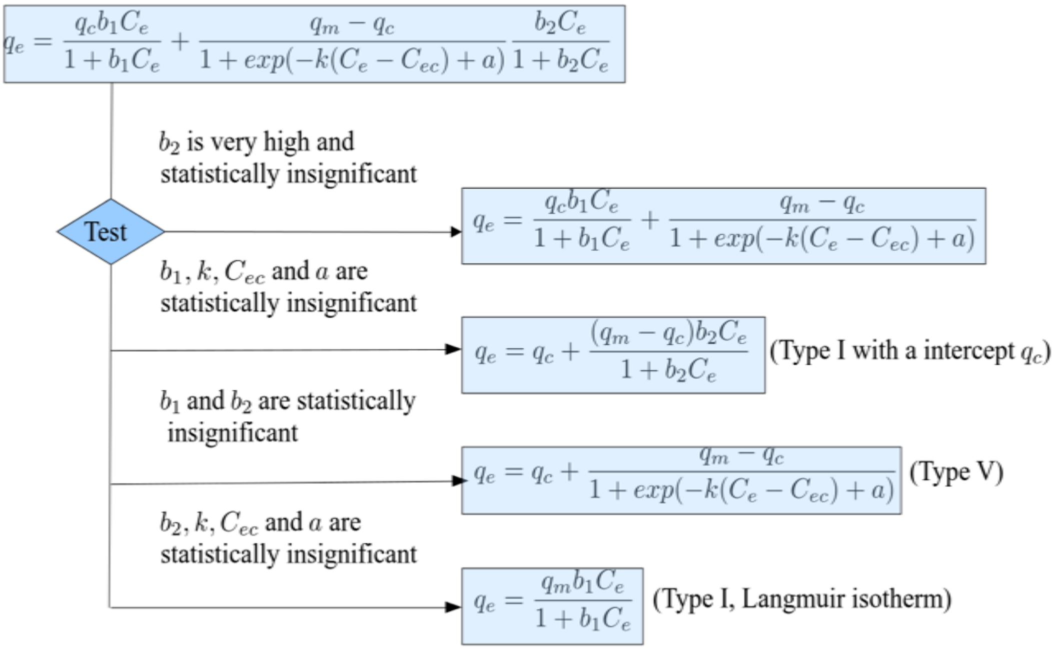

Figure 4 A general scheme to obtain a parsimonious model from a general form of the 2-step Langmuir isotherm.

A non-linear least-squares minimization and curve-fitting (QtiPlot) was used for model fitting and parameter estimation. Parameters were tested for significance at a 95 % confidence level using the student's t-distribution with degrees of freedom *n*, *p* where *p* is the number of measurements, and *n* is the number of parameters. For each of experiment, n was 18 (6×3), p was 2 for Langmuir and Freundlich isotherm, and 4 - 5 for other models. The $1 \rightarrow \propto$ confidence interval for the parameter b_i in the model can be calculated as follows:

$$b_i \pm se(b_i) t(n-p; \propto/2) \tag{14}$$

where $t(n-p; \propto/2)$ is the student's t-distribution with *n*, *p* degree of freedom. That is the significant parameter (at a 95 % confidence level) must pass the criterion $b_i/se(b_i) > t(n-p; \propto/2) \simeq 2.0$. Alternatively, the overall model significance can be tested against the following F-distribution.

$$F(p-1, n-p) = \frac{R^2}{1-R^2} \frac{n-p}{p-1} \tag{15}$$

For example, the full-form TSL or TSF isotherm has 7 parameters and the current data set has 21 data points ($p-1 = 6$ and $n-p = 15$). Thus $F > 2.7$ is the criterion for overall model significance at a 95 % confidence level.

Fitting 2-step isotherms to the equilibrium data: A strategy

After extensive trials, the authors proposed the following strategy to obtain parsimonious models and their representations for each set of data.

The traditional Langmuir and Freundlich equations are used to fit the lower parts of the experimental data ($0 < C_e < 100$ ppm) of each data set. This is done to obtain the best isotherm at relatively low As concentration which is in the range of most of the As contamination in most of the mining areas. A statistical analysis was performed to test the significance of the models and their parameters.

If the models and their parameters for the lower part of the isotherm are statistically significant (at the 95 % confidence levels), the 2-step isotherm models are fitted with the full-range data of each data set. The parameters of Langmuir or Freundlich terms of the lower part, which are obtained from step 1, are treated as constants. The statistical analysis is then performed to test the significance of the 2-step model and their parameters.

During the curve fitting for the 2-step model, if some of the parameters are not significant, they are dropped from the model:

1) The 2nd term in the 2-step Langmuir model fitting is not significant (b_2 is not statistically significant) then it is dropped from the model. Similarly, for the 2-step Freundlich model, if the parameter does not pass the significance test, the 2nd Freundlich term is dropped from the model.

2) If the Langmuir and Freundlich parts of the 2nd term are dropped, the only remaining logistic part is used for further data fitting.

3) If both k and a in logistic terms are not statistically significant, then only the 1st term (traditional Langmuir and Freundlich isotherms) will be used to fit the whole range of data.

In this way parsimonious models are obtained for specific cases, while the lower range of As concentration in solution ($0 < C_e < 50$ ppm) is in focus, ensuring its emphasis and accuracy.

The Fe and As densities and the maximum As adsorption capacity (q_m) of sediment

Many previous investigations that the presence of iron oxides, some part of As(V) is reduced to As(III), and then As(III) will form As-Fe complexes on the surface of iron oxide by soil DOM and sulfide. In forming the complexes, Fe(III) is reduced to Fe(II) due to electron transfer, or directly changes to Fe(II) after As(III) combines with the dissolved Fe(III) [10,47,48]. Fe-As-complexation is considered as the main mechanisms for immobilization of As in soils and sediments, which reduces hazards due to the contamination of As in water resources.

Fe-As complex forming and interaction between the Fe-As complex in sediment and As in water involved many factors, particularly pH, temperature, particle sizes and surfaces [10]. Thus, a general prediction of As adsorption dynamics and the relationship at equilibrium was not available, and direct on-site analyses were required. **Table 1** summarizes the analytical results of the sediments sampled from 4 stations along the creek bed.

Table 1 and **Figure 5** show that, the As adsorption capacity (q_m) obtained from the batch experiments at pH 4 and pH 7 were almost identical. It was evident that within pH 4 - 7, pH did not significantly affect q_m of the sediments. It is well known that As adsorption by sediments is enhanced by forming a complex with Fe, Mn and Al. The results in our experiments show that high Fe density tends to be associated with high confirming the previous findings in different sediments.

Table 1 The densities of Fe, As and the maximum As adsorption capacity (q_m) of sediments at different locations along the creek. Background As concentration in the sediment in Ron Phibun district is approximately 30 mg/kg.

Station	Fe (mg/kg)	As (mg/kg)	q_c (mg/kg)			q_m (mg/kg)		
			pH 4	pH 7	pH 12	pH 4	pH 7	pH 12
St1 Huay Huamhuang	719	258	1,216	1,312	50.0	1,753	1,830	1,107
St2 Stadium	917	77	1,284	988	50.0	1,700	1,745	1,528
St3 Huawmhuang-Ronna	924	69	646	804	79.9	2,609	2,539	741
St4 Huay Nam Khun	2,371	106	762	857	243.3	2,601	2,521	922

Note: q_m were obtained from the best-fit adsorption isotherms corresponding to specific sediments.

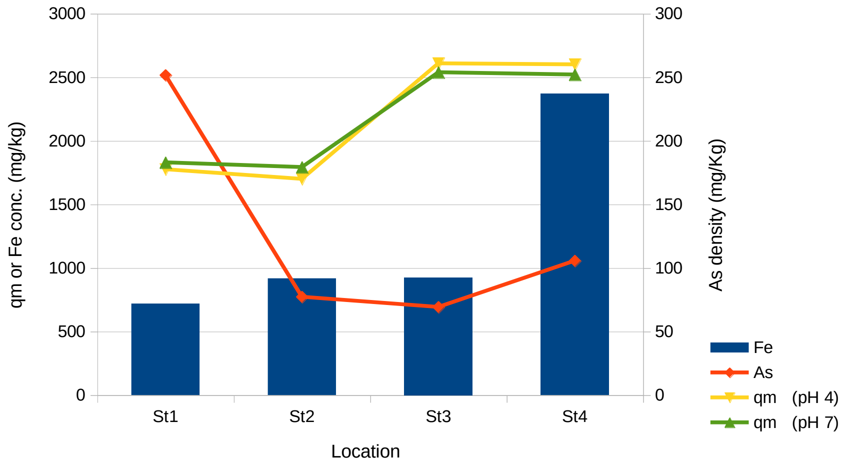

Figure 5 As, Fe densities and As adsorption capacity (q_m) of sediments at 4 different locations along the creek. The distances between St 1 (Huay Huamhuang), St 2 (Stadium), St 3 (Huamhuang-Ronna) and St 4 (Huay Namkhun) are 548, 639, 413 m, respectively.

At St 1 (Huay Huamhuang, which is the beginning of the old mine) which remains on the foot of the hill where experiments started, the As density is as high as 252 mg/kg, despite the fact that the sediment contains relatively low Fe content. This result indicates that the Fe density did not directly affect As density, but tended to correlate with the As adsorption capacity (q_m) instead.

At St 2 (Stadium), 548 m downward from St 1, As density dropped sharply to 69 mg/kg because of continuous As-adsorption as the As-contaminated water was passing through the sediments along the creek bed. In this vicinity, there were not any non-significant As released from the old mine where water previously passed into the stream because it is now a reserved area which is no longer used for mining.

Similarly, as the water continued further to St 3 (639 m downward from St 2) the As density was slightly lower than St 2. Once more, the amount of dissolved As added to the stream was not significant although at St 3 there were a few small old mines which continued to further supply the dissolved As. However, the amount of the As-contaminated water was lower than the rate of As-adsorption occurring in the section of the creek.

At St 4 the sediment had a high level of Fe density (2,371 mg/kg) but a moderate As content (106 mg/kg), showing that, although the high Fe content tended to associate with q_m, it did not affect the As density. In other words, the As transfer between the water phase and the sediment phase is a dynamic phenomenon controlled by many factors including an Fe-As complex forming reaction, an interphase mass transfer, dispersion and the equilibrium relationship of the isotherms.

Further downstream, at St 5 Huay Namchan, St 6 Muang Ngam and St 7 Teppanomchuad Temple, similar levels of Fe appeared (500 - 2,200 mg/kg) in the sediments, however the As levels were at the same level as the background concentration of As in the Ron Phibun area, indicating only mild contamination. Thus, if no As source exists in the area along the creek for more than 3 km to feed the As into the water stream, the sediments can provide a sufficient natural barrier to bar As contamination from entering the water stream, thus bringing the As concentration to a safe level for human and animals.

Kinetics of batch As adsorption/adsorption: Effect of pH

The kinetics of batch As-adsorption/desorption can be modeled as a 1st-order kinetics approximately, although sufficient data in the early adsorption processes are lacking because the adsorption process took place too quickly. It took less than 10 min for the adsorption process to reach a pseudo-equilibrium, thus detailed adsorption kinetics during the transient periods were not observed. However, a 1st-order assumption serves the purpose of the experiments adequately (to find the final equilibrium concentration for each condition).

In general, sediments from all 4 stations behaved at equilibrium similarly, although the concentrations at equilibrium were localized to specific locations. pH slightly affected the isotherm in the pH range of 4 - 7 where the sediments, exhibiting high adsorption capacity (1,500 - 2,900 mg As/kg). However, at pH 12 adsorption shifted towards As dissolution into water, contaminating the water source up to very dangerous levels (> 10 ppm) while the As adsorption capacity of the sediments dropped sharply. This is because at high pH levels, arsenic exists in its ionic form (As $(OH)_3$), which is more soluble than its elemental or non-ionic form (As). Therefore, higher pH levels result in higher solubility of arsenic, making it more likely to dissolve in water.

When plotting the equilibrium data adsorption as shown in **Figures 6 - 9**, it appeared that the adsorption isotherms of the sediments from St 1 (Huay Haumhuang) and St 2 (Stadium) in the pH range of 4 - 7 followed a 2-step trend. However, the adsorption isotherms of the sediments from St 3 (Huamhuang-Ronna) and St 4 (Huay Namkhun) seemed to follow Type V pattern of IUPAC. At the lower ends of the isotherms, the sediments from St 3 and St 4 tended to have a stronger adsorption affinity such that the slope $\partial q_e/\partial C_e$ of the lower ends of the isotherms are very steep, and almost touch the q_e-axis as $C_e \rightarrow 0$.

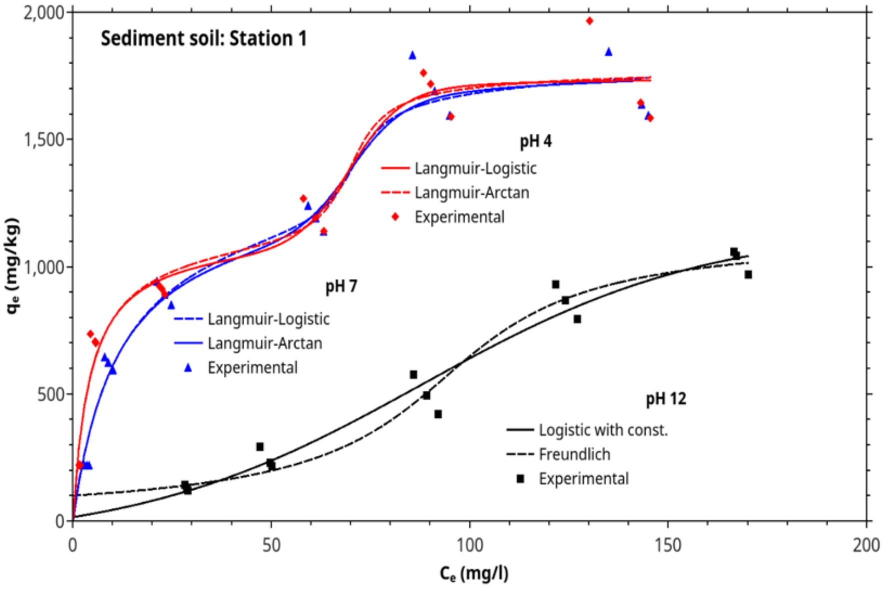

Figure 6 Adsorption isotherms of As in the water-sediment system at St 1 (Huay Huamhuang). The station is located at the mineral preparation area of the old abandoned mines.

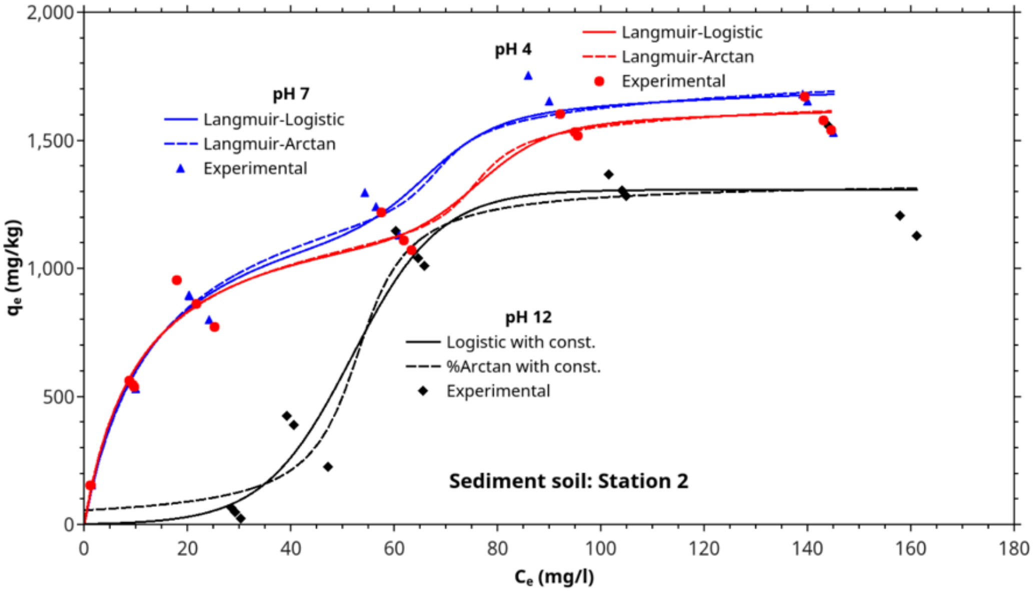

Figure 7 Adsorption isotherms of As in the water-sediment system at St 4 (Huay Namkhun). This station is located 413 m downward from St 3 (Huawmhuang-Ronna). The sediment in this area contained a high level of Fe mineral (2,371 mg Fe/kg) and moderate As content (105.7 mg As/kg). It is a reserved area without any recognizable old mine.

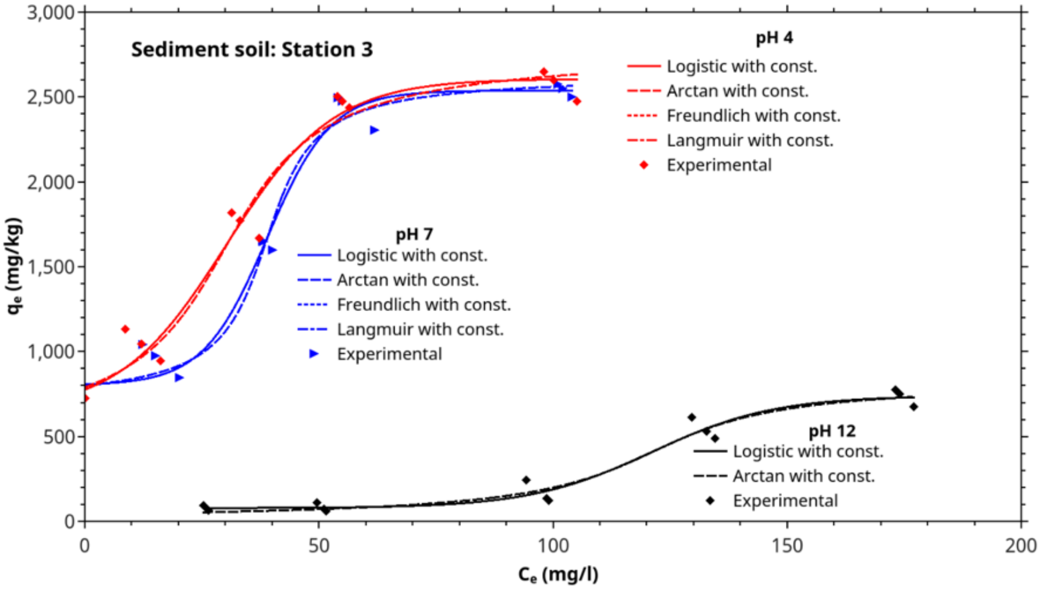

Figure 8 Adsorption isotherms of As in the water-sediment system at St 3 (Huamhuang-Ronna). This station is located 639.2 m downward from St 2 (Stadium). There are a few small/closed old mines around the station, although they were not heavily mined in comparison to St 1.

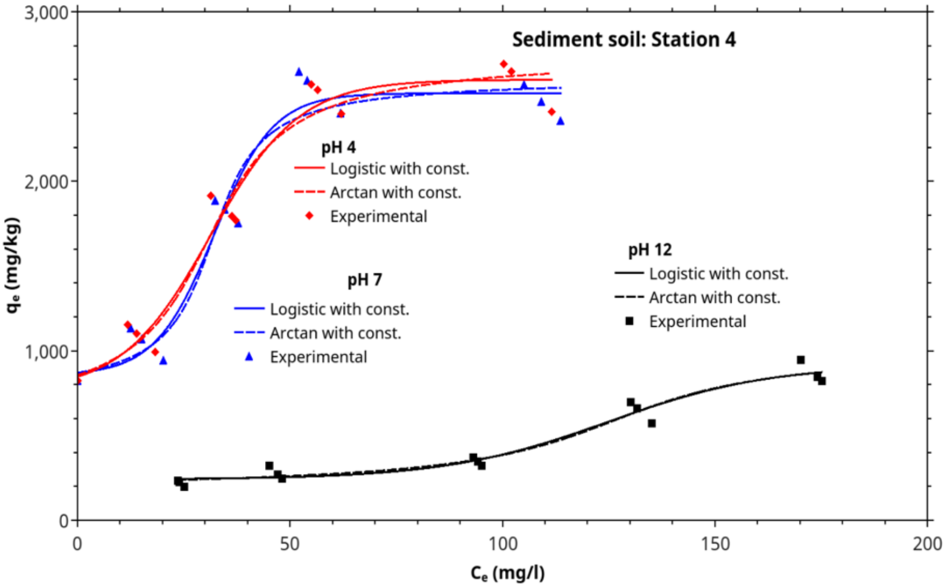

Figure 9 Adsorption isotherms of As in the water-sediment system at St 4 (Huay Namkhun). This station is located 413 m downward from St 3 (Huawmhuang-Ronna). The sediment in this area contained a high level of Fe mineral (2,371 mg Fe/kg) and moderate Ae content (105.7 mg As/kg). It is a reserved area without any recognizable old mine.

Adsorption isotherm of As in water-sediments: Effects of pH (4, 7 and 12)

Following the method outlined in sections 3.4 and 3.5, parsimonious models were obtained for each location and pH as shown in **Figures 5 - 8**. The parameters are summarized in **Tables 2** and **3**.

In all cases the 2nd terms of both the TSL and TSF models and parameter *a* in the Logistic were dropped because they were not statistically significant. Furthermore, except for sediments from St 1 and St 2 at pH 4 - 7, the 1st terms of both the TSL and TSF models were also dropped and replaced by a constant (Logistic or Arctan models with a constant).

pH as high as 12 is unusual in the As-contaminated water in the creek in the Ron Phibun area. However, if the pH is higher than 7, as the pH increases so does the solubility of As in water which needs to be avoided.

All parameters of the 2-step models for 4 different sediments collected from different locations had similar adsorption characteristics, but highly pH dependent when the pH of contaminated water was much higher than 7. Firstly, for pH 4 - 7, if the As concentration in the sediment does not exceed the lower plateau (q_c), they behave as strong adsorbents as indicated by very high b_1 or m for LL and FL isotherms, respectively. Then, secondly, if the As concentration in the sediment exceeds that of the lower plateau but does not exceed the saturation point (q_m), the sediments change gradually from strong to weak adsorbents as the As concentration in the solid increases. If the sediment approaches the maximum capacity (q_m) and the As concentration in water is high enough ($C \gg C_{ec}$), the adsorption will cease. However, if As concentration in the water is in the neighborhood of C_{ec} or lower, As will be desorbed from the sediment and dissolve into the water.

The effect of pH on adsorption capacity of As(V) and As(III) is complex, and was described by many authors [42,49,50,51]. Under acidic (pH and lt; 4) and basic (pH and gt; 7.5) conditions the capacity is low because of material dissolution (pH and lt; 4) and OH--Fe-complex competition (pH and gt; 7.5) for As(V) and As(III).

Under acidic conditions (4 and lt; pH 7), there was excess H+ on the surface of adsorbents (soils or sediment containing Fe-complexes), which tended to fix of H2 AsO −4 and HAsO2 −4 by electrostatic force and complexation. When pH increased, the functional groups on the soils or sediment surface lost more proton, opposing the adsorption of oxygen-containing As anions [42,49]. The results in our current work agree well with most of the previous work, albeit some variation due to the specific nature of the soils and sediments in Ron Phibun region, Thailand.

Table 2 Summary description of the 2-step Langmuir and Freundlich isotherms, parameters and R^2 at St1 (Huay Huawmheang) and St 2 (Stadium).

Model	**Parameter**	**Huay Huawmeang**			**Stadium**		
		pH 4	**pH 7**	**pH 12**	**pH 4**	**pH 7**	**pH 12**
Langmuir-Logistic Isotherm	C_{ec} (ppm)	73.1	70.12	90.5	76.2	55.0	51.7
	b_1(kg/mg)	0.103	0.087	-	0.092	0.135	-
	κ_l(ppm)	0.140	0.15	0.033	0.15	0.117	0.118
	q_m(mg/kg)	1,753	1,830	1,107	1,700	1,745	1,528
	q_c(mg/kg)	1,216	1,312	-	1,284	981	-
	Adjusted R^2	0.985	0.976	0.968	0.985	0.982	0.944
Freundlich-Logistic Isotherm	C_{ec} (ppm)	73.1	73.1	-	73.1	39.8	-
	m	5.52	2.72		2.62	2.17	
	κ_l (ppm)	0.15	0.140		0.140	0.15	
	q_m (mg/kg)	993	267		267	277	
	q_c (mg/kg)	542	258		252	181	
	Adjusted R^2	0.964	0.971		0.971	0.946	
Langmuir-Arctan Isotherm	C_{ec} (ppm)	68.4	70.6	94.0	75.5	68.1	52.9
	b_1 (kg/mg)	0.210	0.080	-	0.090	0.070	-
	κ_l (ppm)	0.281	0.15	0.037	0.15	0.15	0.117
	q_m (mg/kg)	1,780	1,863	1,140	1,718	1,831	1,341
	q_c (mg/kg)	1,164	1,324	-	1,260	1,416	-
	Adjusted R^2	0.968	0.976	0.964	0.985	0.982	0.942
Freundlich-Arctan Isotherm	C_{ec} (ppm)	73.3	-	-	-	-	-
	m	5.67	2.47				
	κ_l (ppm)	0.15	-				
	q_m (mg/kg)	1052	-				
	q_c (mg/kg)	538	236				
	Adjusted R^2	0.968	0.967				

Model	Parameter	Huay Huawmeang			Stadium		
		pH 4	pH 7	pH 12	pH 4	pH 7	pH 12
Langmuir (lower range)	b_1 (kg/mg)	0.243	0.0715	-	0.103	0.135	-
	q_c (mg/kg)	1,111	1,452		1,216	981	
	Adjusted R^2	0.951	0.976		0.957	0.992	
Freundlich (lower range)	m	3.74	2.72	0.899	2.62	2.17	-
	q_c (mg/kg)	393	258	3.72	252	181	
	Adjusted R^2	0.943	0.958	0.968	0.954	0.978	

Table 3 Summary of the 2-step Langmuir and 2-step Freundlich isotherms, parameters and the best-fit parameters (R^2) at St 3 (Huawmhuang-Ronna) and St 4 (Huay Namkhun).

Model	Parameter	Huawmhuang-Ronna			Huay Namkhun		
		pH 4	pH 7	pH 12	pH 4	pH 7	pH 12
Logistic with const	C_{ec} (ppm)	30.0	38.8	121	31.2	32.1	124
	b_1 (kg/mg)						
	κ_l (ppm)	0.087	0.146	0.076	0.095	0.144	0.052
	q_m (mg/kg)	2,609	2,539	741	2,601	2,521	921
	q_c (mg/kg	646	803	79.9	762	857	243
	Adjusted R^2	0.965	0.972	0.952	0.957	0.947	0.947
Arctan with const	C_{ec} (ppm)	29.8	38.7	122	30.6	31.7	126
	b_1 (kg/mg)						
	κ_l (ppm)	0.065	0.133	0.061	0.071	0.119	0.036
	q_m (mg/kg)	2,786	2,638	800	2,759	2,615	1,015
	q_c (mg/kg	438	681	32.0	557	715	168
	Adjusted R^2	0.959	0.973	0.952	0.951	0.937	0.948

Conclusions

Two-step Langmuir/Freundlich models were established for the sorption isotherms of As contamination in the sediments at the old tin-mine areas in Ron Phibun district, Nakhon Si Thammarat province. However, heavy metal contamination in the natural environment is complex. Specific cases require corresponding sets of data and appropriate models to be used in studies. Furthermore, if quantitative description and prediction is the main objective, appropriate transport-phenomena models must be developed and used for the specific cases. For example, the isotherms reported in this work were developed for the sediment soils found in this area. It is expected to be applicable for similar environments although additional adsorption experiments should be carried out to re-calibrate the isotherm models.

References

[1] H Jones, P Visoottiviseth, MK Bux, R Födényi, N Kováts, G Borbély and Z Galbács. Case reports: Arsenic pollution in Thailand, Bangladesh, and Hungary. *Rev. Environ. Contam. Toxicol.* 2009; **197**, 163-87.

[2] Y Yang, X Rao, Q Fu, X Zhang, J Gao, X Wan, J Zhu, G Huang and H Hu. The inhibiting effects of organic acids on arsenic immobilization by ferrihydrite: Gallic acid as an example. *Chemosphere* 2022; **299**, 134286.

[3] U Siripitayakunkit, P Visudhiphan, M Pradipasen and T Vorapongsathron. *Association between chronic arsenic exposure and children's intelligence in Thailand*. *In*: WR Chappell, CO Abernathy and RL Calderon (Eds.). Arsenic exposure and health effects III. Elsevier Science Ltd, Oxford, 1999, p. 141-9.

[4] M Williams, F Fordyce, A Paijitprapapon and P Charoenchaisri. Arsenic contamination in surface drainage and groundwater in part of the southeast Asian tin belt, Nakhon Si Thammarat Province, southern Thailand. *Environ. Geol.* 1996; **27**, 16-33.

[5] TM Williams, BG Rawlins, B Smith and M Breward. *In-vitro* determination of arsenic bioavailability in contaminated soil and mineral beneficiation waste from Ron phibun, southern Thailand: A basis for improved human risk assessment. *Environ. Geochem. Health* 1998; **20**, 169-77.

[6] K Sripaoraya, W Siriwong, S Pavittranon and R Chapman. Environmental arsenic exposure and risk of diabetes type 2 in Ron Phibun subdistrict, Nakhon Si Thammarat Province, Thailand: Unmatched and matched case-control studies. *Risk Manag. Healthc. Pol.* 2017; **10**, 41-8.

[7] Y Cai, Y Mi, J Yu and H Zhang. Arsenic speciation and kinetic release simulation of stream sediment contaminated by gold mining. *J. Soils Sediments* 2016; **16**, 1121-9.

[8] SM Azam, TC Sarker and S Naz. Factors affecting the soil arsenic bioavailability, accumulation in rice and risk to human health: A review. *Toxicol. Mech. Meth.* 2016; **26**, 565-79.

[9] PL Smedley and DG Kinniburgh. A review of the source, behavior and distribution of arsenic in natural waters. *Appl. Geochem.* 2002; **17**, 517-68.

[10] X Zhang, H Fan, J Yuan, J Tian, Y Wang, C Lu, H Has and W Sun. The application and mechanism of iron sulfides in arsenic removal from water and wastewater: A critical review. *J. Environ. Chem. Eng.* 2022; **10**, 108856.

[11] M Liu, F Sun, Y Lv, Y Xu, M Li, Y Wang, X Yin and H Jiang. Remediation of arsenic-contaminated soil by nano-zirconia modified biochar. *Environ. Sci. Pollut. Res. Int.* 2021; **28**, 68792-803.

[12] A Deonarine, A Kolker, MW Doughten, JT Holland and JD Bailoo. Mobilization of arsenic from coal fly ash in the presence of dissolved organic matter. *Appl. Geochem.* 2021; **128**, 104950.

[13] JZ Lima, EFD Silva, C Patinha, N Durães, EM Vieira and VGS Rodrigues. Sorption of arsenic by composts and biochars derived from the organic fraction of municipal solid wastes: Kinetic, isotherm and oral bioaccessibility study. *Environ. Res.* 2022; **204**, 111988.

[14] MC Teixeira, AC Santos, CS Fernandes and JC Ng. Arsenic contamination assessment in Brazil - Past, present and future concerns: A historical and critical review. *Sci. Total Environ*. 2020; **730**, 138217.

[15] A Khan, S Khan, M Lei, M Alam, MA Khan and A Khan. Biochar characteristics, applications and importance in health risk reduction through metal immobilization. *Environ. Tech. Innovat*. 2020; **20**, 101121.

[16] Agency for Toxic Substances and Diseases Registry. Toxicological profile for arsenic, Available at: https://www.atsdr.cdc.gov/ toxprofiles/tp2.pdf, accessed October 2023.

[17] Official Journal of the European Union. *Council directive 98/83/EC of 3 November 1998 on the quality of water intended for human consumption*. Official Journal of the European Union, Luxembourg, 1998, p. 32-54.

[18] United States Environmental Protection Agency. 2*018 Edition of the drinking water standards and health advisories tables*. National Service Center for Environmental Publications, Washington DC, 2018.

[19] J Wang, Z Li, Q Zhu, C Wang and X Tang. Review on arsenic environment behaviors in aqueous solution and soil. *Chemosphere* 2023; **333**, 138869.

[20] K Singh, M Agarwal and Renu. Heavy metal removal from wastewater using various adsorbents: A review. *J. Water Reuse Desalination* 2017; **7**, 387-419.

[21] Z Li, X Liu, W Jin, Q Hu and Y Zhao. Adsorption behavior of arsenicals on MIL-101(Fe): The role of arsenic chemical structures. *J. Colloid Interface Sci.* 2019; **554**, 692-704.

[22] H Chen, X Yuan, L Jiang, H Wang and G Zeng. Highly efficient As(III) removal through simultaneous oxidation and adsorption by N-CQDs modified MIL-53(Fe). *Separ. Purif. Tech.* 2022; **286**, 120409.

[23] X Zhao, X Yu, X Wang, S Lai, Y Sun and D Yang. Recent advances in metal-organic frameworks for the removal of heavy metal oxoanions from water. *Chem. Eng. J.* 2021; **407**, 127221.

[24] GA Kloster, M Valiente, NE Marcovich and MA Mosiewicki. Adsorption of arsenic onto films based on chitosan and chitosan/nano-iron oxide. *Int. J. Biol. Macromol.* 2020; **165**, 1286-95.

[25] LN Pincus, PV Petrović, IS Gonzalez, E Stavitski, ZS Fishman, HE Rudel, PT Anastas and JB Zimmerman. Selective adsorption of arsenic over phosphate by transition metal cross-linked chitosan. *Chem. Eng. J.* 2021; **412**, 128582.

[26] X Shi, C Wang, J Zhang, L Guo, J Lin, D Pan, J Zhou, J Fan, T Ding and Z Guo. Zwitterionic glycine modified Fe/Mg-layered double hydroxides for highly selective and efficient removal of oxyanions from polluted water. *J. Mater. Sci. Tech.* 2020; **51**, 8-15.

[27] C Yin, C Wang and Q Hu. Selective removal of As(V) from wastewater with high efficiency by glycine-modified Fe/Zn-layered double hydroxides. *Adv. Compos. Hybrid Mater.* 2021; **4**, 360-70.

[28] IC Yadav, NL Devi and S Singh. Reductive dissolution of iron-oxyhydroxides directs groundwater arsenic mobilization in the upstream of Ganges River basin, Nepal. *J. Geochem. Explor.* 2015; **148**, 150-60.

[29] C Gérente, Y Andrès, G McKay and PL Cloirec. Removal of arsenic(V) onto chitosan: From sorption mechanism explanation to dynamic water treatment process. *Chem. Eng. J.* 2010; **158**, 593-8.

[30] MC Amacher. *Nickel, cadmium, and lead*. *In*: DL Sparks, AL Page, PA Helmke, RH Loeppert, PN Soltanpour, MA Tabatabai, CT Johnston and ME Sumner (Eds.). Methods of soil analysis: Part 3 chemical methods. American Society of Agronomy, Wisconsin, 2018, p. 739-68.

[31] BY Zhu and T Gu. General isotherm equation for adsorption of surfactants at solid/liquid interfaces. Part 1. Theoretical. *J. Chem. Soc. Faraday Trans 1 Phys. Chem. Condens. Phases* 1989; **85**, 3813-7.

[32] S Kundu, SS Kavalakatt, A Pal, SK Ghosh, M Mandal and T Pal. Removal of arsenic using hardened paste of Portland cement: Batch adsorption and column study. *Water Res.* 2004; **38**, 3780-90.

[33] JG Catalano, Y Luo and B Otemuyiwa. Effect of aqueous Fe (II) on arsenate sorption on goethite and hematite. *Environ. Sci. Tech.* 2011; **45**, 8826-33.

[34] S Dixit and JG Hering. Comparison of arsenic(V) and arsenic(III) sorption onto iron oxide minerals: Implications for arsenic mobility. *Environ. Sci. Tech.* 2003; **37**, 4182-9.

[35] C Tokoro, Y Yatsugi, H Koga and S Owada. Sorption mechanisms of arsenate during coprecipitation with ferrihydrite in aqueous solution. *Environ. Sci. Tech.* 2010; **44**, 638-43.

[36] C Siripatana, H Thongpan and A Promraksa. A generalized volumetric dispersion model for a class of two-phase separation/reaction: Finite difference solutions. *J. Phys. Conf. Ser.* 2017; **820**, 12015.

[37] PR Hesse. *A textbook of soil chemical analysis*. John Murray, London, 1971.

[38] SK Maji, A Pal, T Pal and A Adak. Adsorption thermodynamics of arsenic on laterite soil. *J. Surf. Sci. Tech.* 2007; **22**, 161-76.

[39] DL Johnson and MEQ Pilson. Spectrophotometric determination of arsenite, arsenate, and phosphate in natural waters. *Anal. Chim. Acta* 1972; **58**, 289-99.

[40] KSW Sing, DH Everett, RAW Haul, L Moscou, RA Pierotti, J Rouquerol and T Siemieniewska. Reporting physisorption data for gas/solid systems with special reference to the determination of surface area and porosity (recommendations 1984). *Pure Appl. Chem.* 1985; **57**, 603-19.

[41] M Mourabet, HE Boujaady, AE Rhilassi, H Ramdane, M Bennani-Ziatni, RE Hamri and A Taitai. Defluoridation of water using Brushite: Equilibrium, kinetic and thermodynamic studies. *Desalination* 2011; **278**, 1-9.

[42] K Iamsaard, CH Weng, LT Yen, JH Tzeng, C Poonpakdee and YT Lin. Adsorption of metal on pineapple leaf biochar: Key affecting factors, mechanism identification, and regeneration evaluation. *Bioresource Tech.* 2022; **344**, 126131.

[43] S Rahdar, M Taghavi, R Khaksefidi and S Ahmadi. Adsorption of arsenic (V) from aqueous solution using modified saxaul ash: Isotherm and thermodynamic study. *Appl. Water Sci.* 2019; **9**, 87.

[44] SA Chaudhry, Z Zaidi and SI Siddiqui. Isotherm, kinetic and thermodynamics of arsenic adsorption onto Iron-Zirconium Binary Oxide-Coated Sand (IZBOCS): Modelling and process optimization. *J. Mol. Liq.* 2017; **229**, 230-40.

[45] D Kucharavy and RD Guio. Application of S-shaped curves. *Procedia Eng.* 2011; **9**, 559-72.

[46] A Tsoularis and J Wallace. Analysis of logistic growth models. *Math. Biosci.* 2002; **179**, 21-55.

[47] CB Tabelin, RD Corpuz, T Igarashi, M Villacorte-Tabelin, RD Alorro, K Yoo, S Raval, M Ito and N Hiroyoshi. Acid mine drainage formation and arsenic mobility under strongly acidic conditions:

Importance of soluble phases, iron oxyhydroxides/oxides and nature of oxidation layer on pyrite. *J. Hazard. Mater.* 2020; **399**, 122844.

[48] S Park, SH Kim, H Chung, J An and K Nam. Effect of organic substrate and Fe oxides transformation on the mobility of arsenic by biotic reductive dissolution under repetitive redox conditions. *Chemosphere* 2022; **305**, 135431.

[49] ZH Khan, M Gao, W Qiu, M Qaswar, MS Islam and Z Song. The sorbed mechanisms of engineering magnetic biochar composites on arsenic in aqueous solution. *Environ. Sci. Pollut. Res. Int.* 2020; **27**, 41361-71.

[50] World Health Organization. Guidelines for drinking-water quality, Available at: https://www.who.int/publications/i/item/9789241549950, accessed October 2023.

[51] Z Ha, M Ma, X Tan, Y Lan, Y Lin, TC Zhang and D Du. Remediation of arsenic contaminated water and soil using mechanically (ball milling) activated and pyrite-amended electrolytic manganese slag. *Environ. Res*. 2023; **234**, 116607.